Eur. Phys. J. D **12**, 147–151 (2000)

THE EUROPEAN
PHYSICAL JOURNAL D
EDP Sciences

Electric dipole moment and charge transfer in alkali-C_{60} molecules

R. Antoine[a], D. Rayane, E. Benichou, Ph. Dugourd, and M. Broyer

Laboratoire de Spectrométrie Ionique et Moléculaire[b], Université Lyon I et CNRS, 43 boulevard du 11 novembre 1918, 69622 Villeurbanne Cedex, France

Received 3 March 2000 and Received in final form 26 April 2000

Abstract. We have measured the electric dipole moment of isolated alkali-C_{60} molecules (with alkali = Li, Na, K, Rb, and Cs) by molecular beam deflection experiments. The dipole increases from 12.4 D for LiC_{60} to 21.5 D for CsC_{60}. These results are compared to those deduced from an analytical polarizable-ion model. This comparison shows that there is a strong electron transfer from the alkali atom to the C_{60} cage, which is almost complete for KC_{60} and RbC_{60}.

PACS. 33.15.Kr Electric and magnetic moments (and derivatives), polarizability, and magnetic susceptibility – 34.70.+e Charge transfer – 61.48.+c Fullerenes and fullerene-related materials

1 Introduction

Since the discovery of synthetic routes for isolating macroscopic amounts of C_{60} molecules [1], a lot of works have been devoted to study their chemical and physical properties. It has been demonstrated that C_{60} films become conductive and even superconductive at low temperature, when doped with alkali metal atoms [2,3]. The fullerene cage easily accommodates excess charges from outer or inner metal atoms. A remarkable example concerns the K_6C_{60} solid, where a six time negatively charged C_{60} molecule is predicted [4]. These spectacular results have initiated numerous theoretical and experimental works on isolated endohedral or exohedral metallofullerenes (metal atoms respectively inside and outside the carbon cage). For endohedral species, calculations predict a total electron transfer from the metal atom to the C_{60} cage [5–8]. For exohedral species, an accurate prediction of charge transfer is more difficult [9]. The main difficulty to perform *ab initio* calculations on exohedral systems, arises from the fact that the equilibrium distance between the metal atom and the C_{60} cage is large. An extended basis set is required to reproduce correctly the charge transfer between the carbon cage and the alkali atom [10].

Martin and collaborators have performed an extensive study of metal-coated fullerenes in the gas phase, observing electronic and geometric shells [11]. Photoelectron spectroscopy experiments have shown that a strong charge transfer occurs in isolated sodium and potassium-coated C_{60} molecules [12,13]. Low-energy scattering of alkali atoms on C_{60} fullerenes have also led to valuable quantitative data for unbound system [14,15]. The interpretation of these collision experiments with simple analytical models have allowed to describe the long-range interaction in these systems. However, up to now, almost no quantitative experimental results are available on the electronic properties of a M–C_{60} molecule, in particular on the interaction between the metal atom and the fullerene cage.

In this article, we present the measurement of the permanent dipole moment of isolated alkali-C_{60} molecules by molecular beam deflection technique [16]. The electric dipole moment is a direct observable of the charge transfer which occurs between the C_{60} molecule and the alkali atom. We present the experimental set-up and the experimental results in Sections 2 and 3. In Section 4, the charge transfer is discussed and the data are compared to the results of an analytical polarizable-ion model, that allows one to calculate dipole moments of alkali-C_{60} in their ionic configuration.

2 Experimental

The experimental molecular beam deflection apparatus has been already described in details [17]. The alkali M–C_{60} clusters are produced by laser vaporization of a rod made of ≈ 80% of alkali halide salt (LiCl, NaCl, KBr, RbI, and CsCl) and ≈ 20% of purified C_{60} powder (> 99.9% purchased from MER corp.). We use the third harmonic of a Nd:YAG to vaporize the rod and Neon as carrier gas. A low laser power is used in order to avoid any fragmentation of the fullerenes. With the low laser power that we are using for the vaporization, the transfer of the alkali

---

[a] e-mail: `antoine@lasim.univ-lyon1.fr`

[b] UMR 5579 du CNRS

atom inside the cage can be excluded. The M–C_{60} compounds correspond to exohedral alkali fullerene molecules. The clusters leave the source through a 5 cm-long nozzle. The temperature of the nozzle can be adjusted from 150 K to 500 K. The molecular beam is skimmed and tightly collimated by two slits. It is deflected in a "two-wire" electric field configuration. The clusters are ionized 1 m after the deflector in the extraction region of a position-sensitive time of flight mass spectrometer. The deviation d of a M–C_{60} molecule, is determined by comparing the arrival time at the detector measured with the electric field in the deflector to the arrival time measured without electric field in the deflector. In first approximation, the difference in time Δt is proportional to d. The deviation d for a given molecule of mass m with an average polarizability α and a velocity v is given by:

$$d = \frac{\alpha K F \dfrac{\partial F}{\partial z}}{2 m \nu^2} \tag{1}$$

where K is a geometric factor. F, $\partial F/\partial z$ are respectively the field and the gradient of the electric field in the deflector. The velocity is selected and measured with a mechanical chopper.

3 Electric dipole moment of alkali-C_{60} molecules

Figure 1 shows typical arrival time distribution (ATD) profiles of RbC_{60} measured with and without electric field in the deflector (24 kV and 0 kV) at two different temperatures. At T = 289 K, both ATD profiles are nearly symmetrical. The profile obtained with the electric field in the deflector is time shifted toward longer times of flight. This global shift corresponds to a static polarizability equal to ~ 2485 $Å^3$ for all the molecules. At lower temperature (T = 183 K), an additional broadening of the profile is observed when the electric field in the deflector is turned on. All the molecules in the beam do not have the same polarizability α. The small oscillations observed on the signal are due to ions with slightly different masses. The polarizabilities, calculated using equation (1) and the average deviation measured in ATD, are reported in Figure 2 as a function of the inverse of the temperature. Experiments were performed with a voltage across the deflector of 24 kV and for a nozzle temperature in the range of 150–500 K. In the range of hot temperatures, the evolution of the polarizability of RbC_{60} and NaC_{60} is linear with respect to the inverse of the temperature. In the range of cold temperatures, the profiles are broadened (see Fig. 1) and the average polarizability does not follow the linear behavior.

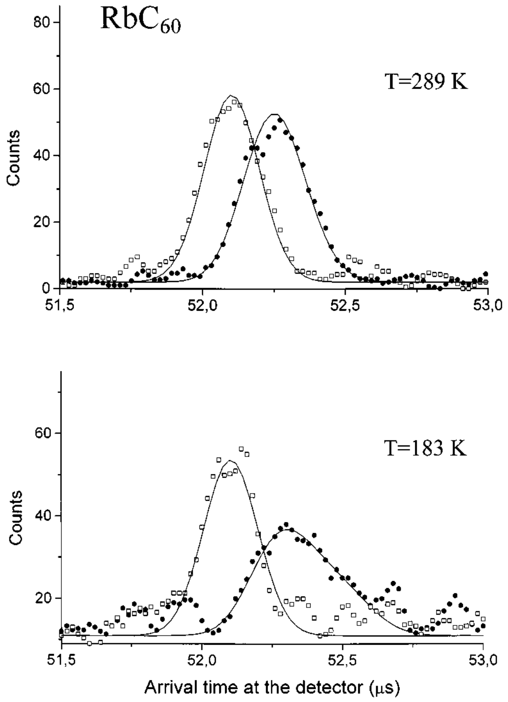

Fig. 1. Experimental arrival time distribution (ATD) profiles of RbC_{60} molecules at two different temperatures. (□) Experimental profiles without electric field in the deflector, (●) experimental profiles with electric field in the deflector (24 kV); (———) results of simulations.

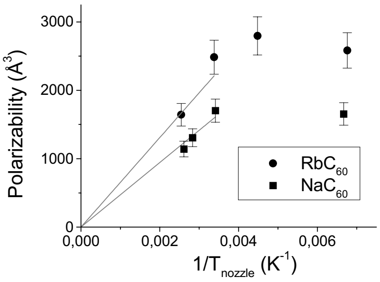

Fig. 2. Temperature dependence of the polarizability of RbC_{60} and NaC_{60} molecules. The temperature of the nozzle has been varied from 150 K to 500 K. The solid line represents a linear fit on the first three reported data.

Recently, we have shown that, for KC_{60} molecules, there is a strong permanent dipole μ along the direction joining the center of the cage to the alkali atom [16]. At room temperature, the alkali atom, and then the direction of the electric dipole moment, can move freely on the surface of the cage. Without electric field, the average value of the dipole is zero. In a static electric field, the dipole is statistically oriented toward the direction of the electric field (paraelectricity). The average value of the dipole is inversely proportional to the temperature, and is given, in first approximation by the Langevin formula. All the molecules are deviated by the same amount, which is proportional to $\alpha = \mu^2/3kT$. Experimental data recorded at $T > 293$ K are in agreement with the linear behavior predicted for a paraelectric system.

As the temperature decreases, the hopping frequency of the alkali atom decreases and the effect of the rotation on the polarizability cannot be neglected. The polarizability of a rotating alkali-C_{60} molecule in a static electric field

Table 1. Experimental permanent dipole moment ($\mu_{\rm exp}$) obtained from deviation measurement and calculated dipole moment ($\mu_{\rm ion}$) of alkali-C_{60} at the minimum of the ionic state curve (see Eq. (3)).

	LiC_{60}	NaC_{60}	KC_{60}	RbC_{60}	CsC_{60}
$\mu_{\rm exp}$(D)	12.4±2.0	16.3±1.6	21.5±2.2	20.6±2.1	21.5±2.2
$\mu_{\rm ion}$(D)	20.1	21.5	24.1	24.3	

Table 2. Lennard-Jones potential parameters.

	LiC_{60}	NaC_{60}	KC_{60}	RbC_{60}
C_6 (10^3 au)	7.92	8.64	12.50	13.40
C_{12} (10^9 au)	76.51	101.81	178.54	192.09

is given by [18,19]:

$$\alpha = \frac{\mu^2}{3kT}\frac{1+\cos^2(\theta)\Omega^2\tau^2}{1+\Omega^2\tau^2} \qquad (2)$$

where Ω and θ are respectively the angular velocity of the molecule and the angle between the molecular angular momentum axis and the axis of the electric field. τ is the characteristic relaxation time due to the hopping of the metal on the C_{60} cage. Experimental profiles are fitted using equations (1, 2), for every accessible value of θ with a weight equal to $2\pi\sin(\theta)$. The rotation energy is taken equal to $(3/2)kT$. The same value of μ is used for all temperatures, the value of τ is adjusted for every temperature. The fits shown in Figure 1 for RbC_{60} (full lines) are obtained for $\mu = 20.6$ D. τ follows an Arrhenius law with an activation energy equal to 0.02 eV. Very low surface diffusion barrier are also observed and calculated for alkali atoms on graphite [20,21]. The upper limit calculated in reference [21] for the diffusion of K atom on graphite is 0.08 eV.

Experimental dipole moments for LiC_{60}, NaC_{60}, KC_{60}, and CsC_{60} obtained with the fitting procedure described above are listed in Table 1. The dipole moment increases with the size of the alkali atom; from 12.4 D for LiC_{60} to 21.5 D for CsC_{60} [22]. Simple physical aspects may explain this behavior. First, alkali atomic and ionic radii increase continuously from lithium to cesium. This induces an increase of the equilibrium distance between the alkali atom and the C_{60} cage. Second, the electropositivity of alkali increases from lithium to cesium. In the frame of the Pauling model for ionic bonds, this is expected to induce an increase of the electron transfer from the alkali to the C_{60}. Both effects will lead to an increase of the dipole moment.

4 Discussion

To analyze these results, one needs to know the relevant interaction forces which bind the alkali atom to the C_{60} cage. For this purpose, we propose to model the alkali-C_{60} system as a donor (alkali atom) and an acceptor (C_{60} cage). The bond in the alkali-C_{60} molecules will be the result of the interaction of the covalent ($V_{\rm cov}$) and the ionic ($V_{\rm ion}$) states. One can have a crude estimate of the potential curves of these states, using a simple analytical expansion of the potentials in power of the inverse interatomic distance (C_n/r^n) [23–25]. We describe the covalent state of the alkali-C_{60} molecules by a Lennard-Jones potential. The ionic state will be given by the sum of a Coulombic ($-C_1/r$), a polarization ($-C_4/r^4$) and a short-range repulsion (C_{12}/r^{12}) terms. The detail of these potentials and the constants that we have used, are given in Appendix A and Table 2.

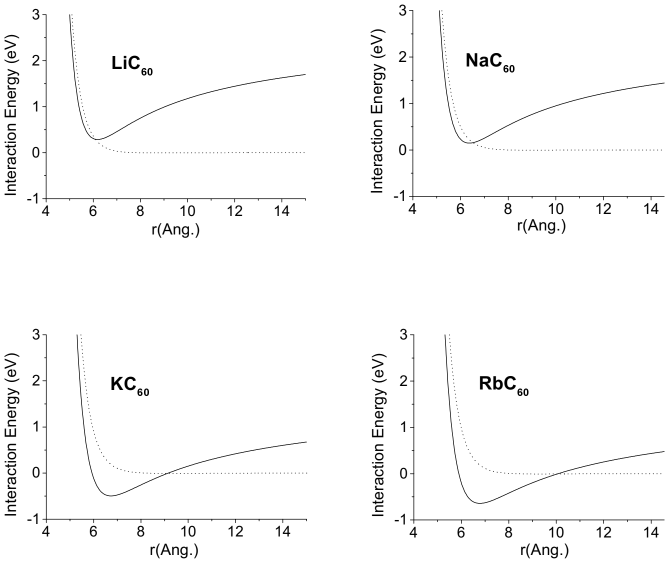

Fig. 3. Ionic (solid line) and covalent (dotted lines) states of LiC_{60}, NaC_{60}, KC_{60} and RbC_{60} molecules (see Appendix A). The asymptotic values of the two states are separated by the difference between the ionization potential of the alkali atom and the electron affinity of C_{60} ($I_{\rm M} - A_{\rm C_{60}}$).

Figure 3 displays the ionic and covalent potentials calculated for LiC_{60}, NaC_{60}, KC_{60} and RbC_{60} using equations (A.1, A.5). The potentials are plotted as a function of the distance between the center of the C_{60} cage and the alkali atom. Their asymptotic values are separated by the difference between the ionization potential of the alkali atom and the electron affinity of C_{60} ($I_{\rm M} - A_{\rm C_{60}}$). The covalent states are weakly bound (5.0–6.4 meV), while the ionic states are strongly bound (2.1–2.4 eV). The curves are similar for all the alkali-C_{60} molecules, but the position in energy of the ionic state with respect to the covalent state strongly depends on the alkali atom. This is due to the strong variation of the value of ($I_{\rm M} - A_{\rm C_{60}}$) from lithium to rubidium (2.69 eV to 1.48 eV). For KC_{60} and RbC_{60}, the minimum of the ionic state is significantly lower in energy than the minimum of the covalent state. In contrary, for LiC_{60} and NaC_{60}, the minimum of the covalent state is slightly lower in energy than the minimum of the ionic state. The ionic and covalent state curves undergo a diabatic crossing at a distance R_x which varies from 6.1 Å for LiC_{60} to 10.0 Å for RbC_{60}. The distance at the minimum of the ionic curve varies from 6.19 Å for LiC_{60} to 6.79 Å for RbC_{60}. At the minimum of the ionic state, one can calculate the corresponding dipole moment.

Taking into account the polarization contribution, especially the strong polarization of the fullerene cage, the permanent dipole moment is given by [26]:

$$\mu = e\left(r - \frac{\left(\alpha_{C_{60}^-} + \alpha_{M^+}\right) r^4 + 4\alpha_{C_{60}^-}\alpha_{M^+} r}{r^6 - 4\alpha_{C_{60}^-}\alpha_{M^+}}\right). \tag{3}$$

Calculated dipole moments, using equation (3) are given in Table 2.

For KC_{60} and RbC_{60}, calculated dipoles are in relative good agreement with experimental values. This shows that, as expected from Figure 3, there is a strong charge transfer from the alkali atom to the C_{60} cage. The ionic state is the configuration of lowest energy and the permanent dipole is close to the permanent dipole calculated for $M^+C_{60}^-$ with equation (3). In contrary, values obtained from equation (3), for LiC_{60} and NaC_{60} significantly overestimate experimental values. There is not a complete charge transfer. This is in agreement with the prediction of our simple model (see Fig. 3). It is clear from this figure, that an accurate description of the bonding needs to take into account the interaction between the ionic and covalent states. The coupling between these two states will lead to a partial ionic character of the bonding. A partial charge transfer for Na atom and a total charge transfer for heavier alkali atoms have also been observed or calculated for alkali-doped fullerides and alkali atoms on graphite [27,28].

In summary, we have measured the electric dipole moment of isolated alkali MC_{60} molecules (with M = Li, Na, K, Rb, and Cs) by molecular beam deflection experiments. They are in the range 12.4–21.5 D from LiC_{60} to CsC_{60}. These results are in qualitative agreement with a simple analysis of ionic and covalent potential curves for the interaction of the alkali atom with the C_{60} cage. We hope that our results will stimulate the development of models able to correctly describe the interaction of a C_{60} molecule with a metal atom.

The authors wish to thank F. Spiegelmann for fruitful discussions.

Appendix A: Formulas for the ionic and covalent potentials of the alkali-C_{60} molecules

The covalent state of alkali-C_{60} molecules is described by a Lennard-Jones (12-6) potential :

$$V_{\mathrm{cov}} = \frac{C_{12}}{r^{12}} - \frac{C_6}{r^6} \tag{A.1}$$

where r is the distance between the alkali atom and the center of the cage. C_6 and C_{12} are the usual Lennard-Jones parameters. C_6 is calculated using the well-known London dispersion formula [14]:

$$C_6 = \frac{3}{2}\hbar\alpha_{\mathrm{M}}\alpha_{\mathrm{C}_{60}}\frac{\omega_{\mathrm{M}}\omega_{\mathrm{C}_{60}}}{\omega_{\mathrm{M}} + \omega_{\mathrm{C}_{60}}} \tag{A.2}$$

where α and ω are the static polarizabilities and the characteristic dipole transition frequencies, which are available in the literature for the alkali atoms and C_{60} [29]. The parameter C_{12} is extracted from C_6 by:

$$C_{12} = \sigma_{\mathrm{MC}_{60}}^6 C_6 \tag{A.3}$$

where $\sigma_{\mathrm{MC}_{60}}$ is the collision parameter given by the usual combination rule [30]:

$$\sigma_{\mathrm{MC}_{60}} = \frac{1}{2}\left(\sigma_{\mathrm{MM}} + \sigma_{\mathrm{C}_{60}\mathrm{C}_{60}}\right) \tag{A.4}$$

$\sigma_{\mathrm{C}_{60}\mathrm{C}_{60}} = 9.59$ Å [31] and σ_{MM} are deduced from scattering measurements of alkali atom on rare gases ($\sigma_{\mathrm{MM}} =$ 5.85 Å [32], 6.37 Å [33], 6.89 Å [34], and 6.90 Å [33], respectively for Li, Na, K, and Rb). The Lennard-Jones parameters for the alkali-C_{60} systems are listed in Table 2.

The ionic state of alkali-C_{60} molecules is given by a polarizable-ion potential. The potential is described by the sum of a Coulombic, a polarization and a short-range repulsion terms:

$$V_{\mathrm{ion}} = \frac{C_{12}}{r^{12}} - \frac{1}{r} - \frac{\left(\alpha_{C_{60}^-} + \alpha_{M^+}\right)}{2r^4} + I_{\mathrm{M}} - A_{\mathrm{C}_{60}} \tag{A.5}$$

where $\alpha_{C_{60}^-}$ and α_{M^+} are the ion polarizabilities ($\alpha_{M^+} =$ 0.029, 0.179, 0.83, and 1.40 Å^3 [35], respectively for Li^+, Na^+, K^+, and Rb^+). For C_{60}^-, we use the experimental polarizability of the neutral C_{60} fullerene ($\alpha_{C_{60}} =$ 76.5 Å^3 [36]). One would expect the polarizability of C_{60}^- to be slightly higher than the polarizability of C_{60}. This would lower the calculated dipoles. We use the same short-range potential (C_{12}/r^{12}) for the ionic state than for the covalent state. In fact, the short-range interaction parameter is essentially driven by the dimension of the C_{60} cage, which is quite the same for the negatively charged cage. Finally, the asymptotic values of the two states are separated by the difference between the ionization potential of the alkali atom and the electron affinity of C_{60} ($I_{\mathrm{M}} - A_{\mathrm{C}_{60}}$). We did not find reliable experimental values for the collision parameter of Cs–C_{60}.

References

1. W. Krätschmer, L.D. Lamb, K. Fostiropoulos, D.R. Huffman, Nature **347**, 354 (1990).
2. A.F. Hebard, M.J. Rosseinski, R.C. Haddon, D.W. Murphy, S.H. Glarum, T.T.M. Palstra, A.P. Ramirez, A.R. Kortan, Nature **350**, 600 (1991).
3. R.C. Haddon, A.F. Hebard, M.J. Rosseinski, D.W. Murphy, S.J. Duclos, K.B. Lyons, B. Miller, J.M. Rosamilia, R.M. Fleming, A.R. Kortan, S.H. Glarum, A.V. Makhija, A.J. Muller, R.H. Eick, S.M. Zahurak, R. Tycko, G. Daddagh, F.A. Thiel, Nature **350**, 320 (1991).
4. S.C. Erwin, M.R. Pederson, Phys. Rev. Lett. **67**, 1610 (1991).
5. J. Ciosolwski, K. Raghavachari, J. Chem. Phys. **98**, 8734 (1993).
6. J. Liu, S. Iwata, Phys. Rev. B **50**, 5552 (1994).
7. D. Tomanek, Y.S. Li, Chem. Phys. Lett. **243**, 42 (1995).

8. B.I. Dunlap, J.L. Ballester, P.P. Schmidt, J. Phys. Chem. **96**, 9781 (1992).
9. T. Aree, T. Kerdcharoen, S. Hannongbua, Chem. Phys. Lett. **285**, 221 (1998).
10. T. Aree, S. Hannongbua, J. Phys. Chem. A **101**, 5551 (1997).
11. U. Zimmermann, N. Malinowski, A. Burkhardt, T.P. Martin, Carbon **33**, 995 (1995).
12. B. Palpant, A. Otake, F. Hayakawa, Y. Negishi, G.H. Lee, A. Nakajima, K. Kaya, Phys. Rev. B **60**, 4509 (1999).
13. L.-S. Wang, O. Cheshnovsky, R.E. Smalley, J.P. Carpenter, S.J. Hwu, J. Chem. Phys. **96**, 4028 (1992).
14. A.A. Scheidemann, V.V. Kresin, W.D. Knight, Phys. Rev. A **49**, R4293 (1994).
15. V.V. Kresin, V. Kasperovich, G. Tikhonov, K. Wong, Phys. Rev. A **57**, 383 (1998).
16. D. Rayane, R. Antoine, P. Dugourd, E. Benichou, A.R. Allouche, M. Aubert-Frécon, M. Broyer, Phys. Rev. Lett. **84**, 1962 (2000).
17. R. Antoine, D. Rayane, A.R. Allouche, M. Aubert-Frécon, E. Benichou, F.W. Dalby, P. Dugourd, M. Broyer, C. Guet, J. Chem. Phys. **110**, 5568 (1999).
18. D.A. McQuarrie, *Statistical Mechanics* (Harper & Row, New York, 1976).
19. P. Dugourd, R. Antoine, D. Rayane, E. Benichou, M. Broyer, Phys. Rev. A **62**, 011201(R) (2000).
20. F. Ancilotto, F. Toigo, Phys. Rev. B **47**, 13713 (1993).
21. L. Lou, L. Österlund, B. Hellsing, J. Chem. Phys. **112**, 4788 (2000).
22. The values for the permanent dipole moment obtained with the relaxation model are higher by $\sim 20\%$ than values that would be deduced directly from the linear fit shown in Figure 2. The data plotted in Figure 2 are obtained by measuring the average deviation of the profile. They do not take into account relaxation effects.
23. V. Aquilanti, D. Cappelletti, F. Pirani, Chem. Phys. **209**, 299 (1996).
24. K.T. Tang, J.P. Toennies, J. Chem. Phys. **66**, 1496 (1977).
25. K.T. Tang, J.P. Toennies, J. Chem. Phys. **80**, 3726 (1984).
26. E.S. Rittner, J. Chem. Phys. **19**, 1030 (1951).
27. M.J. Rosseinsky, D.W. Murphy, R.M. Fleming, R. Tycko, A.P. Ramirez, T. Siegrist, G. Dabbagh, S.E. Barrett, Nature **356**, 416 (1992).
28. M.T. Johnson, H.I. Starnberg, H.P. Hughes, Surf. Sci. **178**, 290 (1986).
29. E.J. Reader, C.H. Corliss, *CRC Handbook of Chemistry and Physics* (CRC Press, Boca Raton, FL, 1998).
30. J.O. Hirschfelder, C.F. Curtiss, R.B. Bird, *Molecular theory of gases and liquids* (John Wiley & Sons, Inc., New York, 1954).
31. M.H.J. Hagen, E.J. Meijer, G.C.A.M. Mooij, D. Frenkel, H.N.W. Lekkerkerker, Nature **365**, 425 (1993).
32. E.W. Rothe, P.K. Rol, R.B. Bernstein, Phys. Rev. **130**, 2333 (1963).
33. E. Hundhausen, H. Pauly, Z. Phys. **187**, 305 (1965).
34. E.W. Rothe, R.H. Neynaber, B.W. Scott, S.M. Trujillo, P.K. Rol, J. Chem. Phys. **39**, 493 (1963).
35. C. Kittel, *Introduction to solid state physics* (John Wiley & Sons, Inc., New York, 1976).
36. R. Antoine, P. Dugourd, D. Rayane, E. Benichou, M. Broyer, F. Chandezon, C. Guet, J. Chem. Phys. **110**, 9771 (1999).